Chemical Science

ROYAL SOCIETY OF CHEMISTRY

EDGE ARTICLE

View Article Online
View Journal | View Issue

Cite this: *Chem. Sci.*, 2024, **15**, 1472

All publication charges for this article have been paid for by the Royal Society of Chemistry

Received 27th November 2023
Accepted 19th December 2023

DOI: 10.1039/d3sc06359c

rsc.li/chemical-science

Incorporation of a self-immolative spacer enables mechanically triggered dual payload release†

Yu-Ling Tseng, Tian Zeng and Maxwell J. Robb *

Polymers that release functional small molecules in response to mechanical force are promising materials for a variety of applications including drug delivery, catalysis, and sensing. While many different mechanophores have been developed that enable the triggered release of a variety of small molecule payloads, most mechanophores are limited to one specific payload molecule. Here, we leverage the unique fragmentation of a 5-aryloxy-substituted 2-furylcarbinol derivative to design a novel mechanophore capable of the mechanically triggered release of two distinct cargo molecules. Critical to the mechanophore design is the incorporation of a self-immolative spacer to facilitate the release of a second payload. By varying the relative positions of each cargo molecule conjugated to the mechanophore, dual payload release occurs either concurrently or sequentially, demonstrating the ability to fine-tune the release profiles.

Introduction

Polymers that release functional small molecules in response to mechanical force are promising for a range of applications including catalysis, sensing, and drug delivery.[1–3] In polymer mechanochemistry, small molecule release is accomplished by using mechanical force to drive productive chemical transformations in stress-responsive molecules termed mechanophores, which are incorporated into polymer chains to achieve force transduction.[4–6] Mechanical force is an appealing external stimulus that is routinely applied using a variety of methods including solution-phase ultrasonication, or tension and compression in polymeric materials, which afford spatiotemporal control over mechanophore activation.[7] In the context of molecular release, a recently reported method for activating mechanochemical reactions using biocompatible focused ultrasound under physiological conditions presents exciting opportunities for biomedical applications including drug delivery.[8] These myriad techniques for external mechanochemical activation coupled with the excellent selectivity and control afforded by molecular structure design have attracted significant interest in the development of mechanophores for small molecule release.[9] For example, *gem*-dichlorocyclopropane mechanophores have been designed to release HCl.[10,11] A flex activation strategy has been devised for the liberation of a small molecule furan from an oxanorbornadiene mechanophore[12] and the release of catalytically active N-heterocyclic carbenes from carbodiimide adducts.[13] Mechanophores have also been developed for the release of carbon monoxide,[14,15] metal ions,[16–18] and other specific small molecules.[19,20]

The development of mechanophores that release multiple different payloads, however, is limited. Herrmann and Göstl have developed a mechanophore platform based on a judiciously designed disulfide motif with cargo molecules attached *via* β-carbonate linkages.[21] Mechanical cleavage of the disulfide bond initiates a 5-*exo*-*trig* cyclization with concomitant cargo release. The mechanophore can be assembled in a convergent fashion such that a distinct cargo molecule is appended *via* each carbonate linkage on either side of the mechanically active disulfide bond.[22] Research has leveraged the bifunctional character of this platform to trigger the concurrent release of a drug molecule and a fluorescent reporter, enabling indirect real-time tracking of drug distribution *in vitro* following *ex situ* mechanochemical activation. Combination chemotherapy is another possible application of dual payload release, in which the simultaneous delivery of two or more chemotherapeutic molecules elicits a synergistic therapeutic effect.[23] Despite the advantageous simplicity of the disulfide mechanophore platform, its susceptibility to activation *via* chemical or enzymatic reduction or thiol exchange reactions limits mechanochemical selectivity and payload scope has largely been limited to alcohols and phenols.[24]

Over the past several years, our group has developed a versatile mechanophore platform enabling the mechanically triggered release of functionally diverse small molecules that relies on masked 2-furylcarbinol derivatives.[25–28] Upon mechanochemical activation, the furan–maleimide mechanophore undergoes a formal retro-Diels–Alder reaction to reveal

Division of Chemistry and Chemical Engineering, California Institute of Technology, Pasadena, California 91125, USA. E-mail: mrobb@caltech.edu

† Electronic supplementary information (ESI) available. See DOI: https://doi.org/10.1039/d3sc06359c

a thermally unstable 2-furylcarbinol derivative, which then spontaneously decomposes to release its covalently bound cargo. This general mechanophore design exhibits excellent selectivity and is capable of efficiently releasing a wide range of molecular payloads.[26] In 2021, we described a mechanophore in which an aryloxy substituent is installed at the 5-position of the furan scaffold, serving both as an electron donating group to enhance molecular release and the position of polymer attachment (Scheme 1a).[27] The synthesis of this aryloxy-substituted mechanophore is efficient and scalable, while maintaining competency for the release of phenols and even more challenging arylamine payloads on reasonable timescales. Furthermore, we discovered a unique fragmentation pathway for the 5-aryloxy-substituted 2-furylcarbinol derivative that resulted not only in the release of the intended cargo molecule attached *via* a carbonate or carbamate linker, but also cleavage of the aryloxy group from the furan. We reasoned that attack of the intermediate furfuryl cation by methanol present in solution generated an *ortho* ester analogue that subsequently collapsed to expel the tyrosol derivative. We further hypothesized that this secondary fragmentation process could potentially be exploited to achieve dual cargo release.[29,30]

Here, we leverage the unique fragmentation of this 5-aryloxy-substituted 2-furylcarbinol scaffold by incorporating a self-immolative spacer that enables the mechanically triggered release of two distinct cargo molecules from a single mechanophore (Scheme 1b). Upon mechanochemical activation, the furan–maleimide Diels–Alder adduct is expected to undergo a formal retro-[4 + 2] cycloaddition reaction to reveal an unstable 2-furylcarbinol derivative, which decomposes *via* a furfuryl cation intermediate according to the arrow pushing mechanism shown in Scheme 1 to release the first covalently bound cargo molecule. Further fragmentation unmasks the judiciously designed phenolic spacer, which self-immolates in a 1,6-elimination process and another decarboxylation event to release the second cargo molecule. We characterize the reactivity of this novel mechanophore design through small molecule model experiments, and demonstrate mechanically triggered dual cargo release from polymers upon ultrasound-induced mechanochemical activation. Furthermore, we show that the release profiles for the two different payloads can be substantially modulated by varying their relative attachment position on the mechanophore.

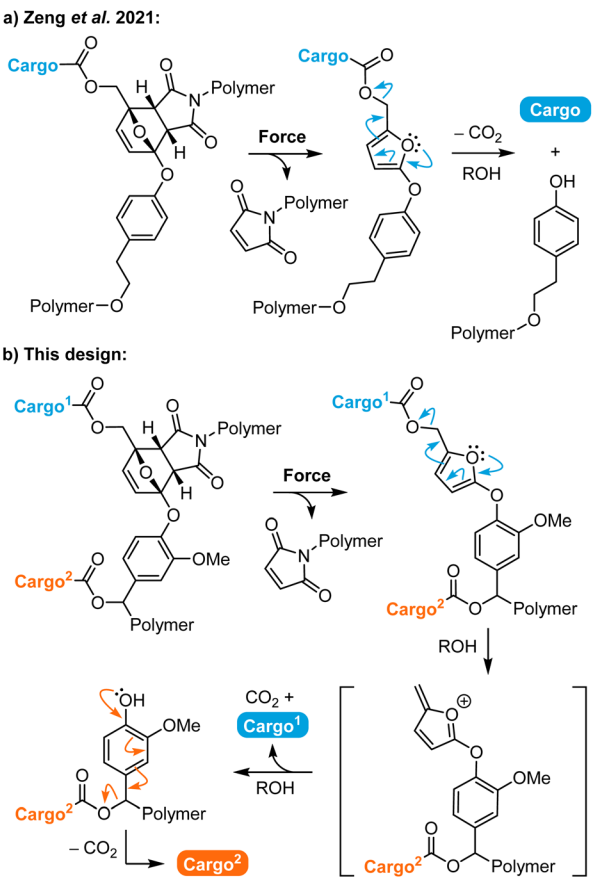

Scheme 1 (a) Mechanically triggered small molecule release is accompanied by a secondary fragmentation pathway resulting in expulsion of a tyrosol-functionalized polymer. (b) Incorporation of a self-immolative spacer enables mechanically triggered dual payload release *via* a multistep retro-Diels–Alder/fragmentation–decarboxylation cascade.

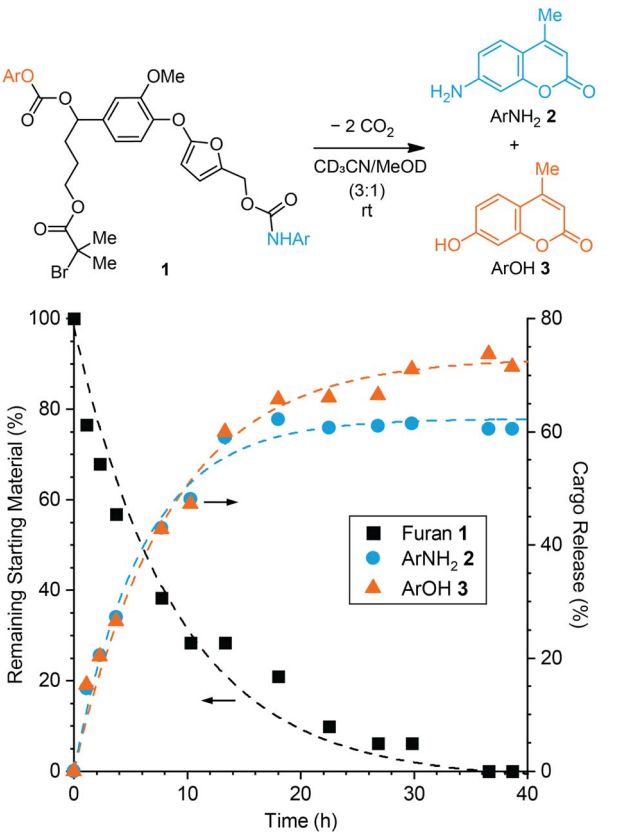

Fig. 1 Reaction of model compound **1** in polar protic solvent at room temperature produces $ArNH_2$ **2** and ArOH **3** *via* a dual fragmentation–decarboxylation cascade. Time-dependent reaction profiles for the conversion of furan **1** and the generation of **2** and **3** characterized by ^1H NMR spectroscopy (3 : 1 MeCN-d_3/MeOD, $[\mathbf{1}]_0$ = 29 mM). A rebound product is also formed under these conditions accounting for an additional ~32% release of $ArNH_2$ **2** as a result of the relatively high substrate concentration (see ESI† for details).

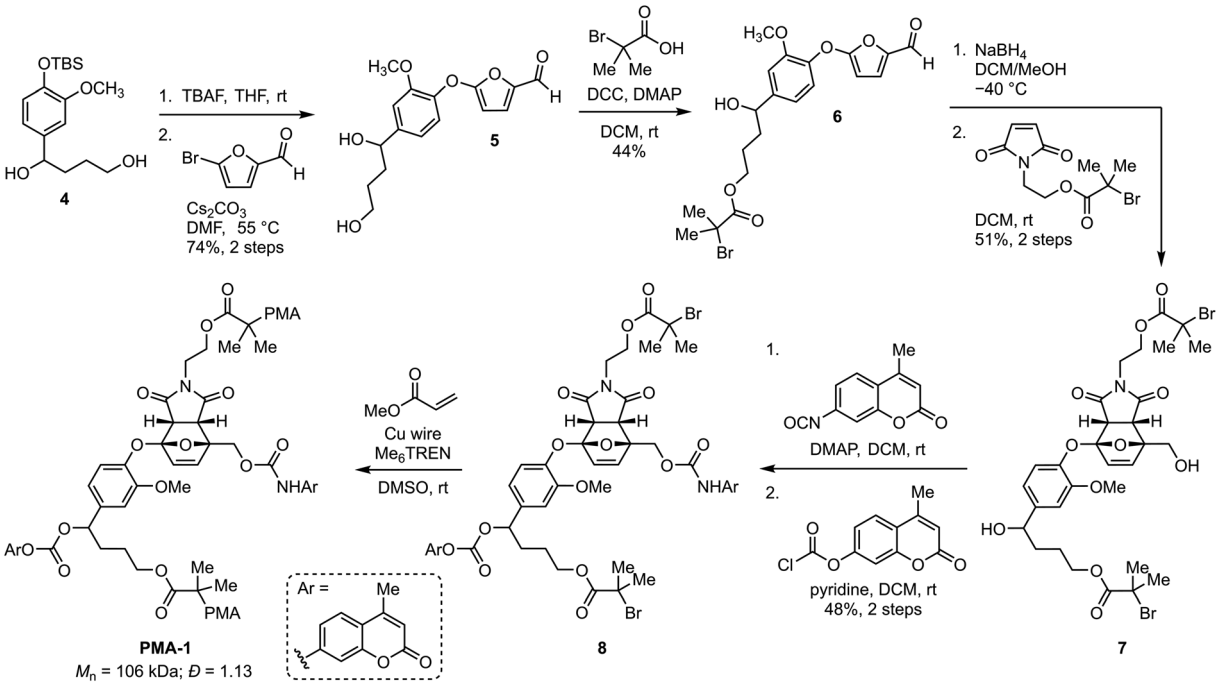

Scheme 2 Synthesis of poly(methyl acrylate) (PMA) polymer **PMA-1** containing a chain-centered mechanophore loaded with two distinct molecular payloads.

Results and discussion

We first investigated the effect of the self-immolative spacer on the decomposition of 5-aryloxy-substituted furan model compound **1** toward dual cargo release. The model compound incorporates an aryloxy substituent derived from vanillin that is capable of a 1,6-elimination mechanism upon expulsion from the furan.[31] For comparison to our prior studies,[26,27] we chose to study the release of fluorogenic aminocoumarin ($ArNH_2$ **2**) and hydroxycoumarin (ArOH **3**) as model payloads, which were connected *via* carbamate and carbonate linkages, respectively (Fig. 1, see the ESI† for synthetic details). Preliminary experiments performed on a simpler 5-aryloxy-substituted furfuryl carbamate compound indicated that both fragmentation processes illustrated in Scheme 1b occur in close succession.[27] Furthermore, the release of phenols *via* 1,6-elimination of similar self-immolative linkers is expected to be faster than the release of an arylamine *via* decomposition of the furfuryl carbamate.[27,32] Therefore we anticipated that the release of $ArNH_2$ **2** and ArOH **3** would occur on similar timescales, with initial decomposition of the 2-furylcarbinol derivative and the release of $ArNH_2$ **2** being rate determining in this case.

Furfuryl carbamate **1** is transiently stable in aprotic solvents like chloroform and acetonitrile; however, the addition of methanol into an acetonitrile solution of the small molecule initiates fragmentation at room temperature resulting in the release of both payloads.[25] To characterize the kinetics of cargo release, model compound **1** was dissolved in CD_3CN followed by addition of CD_3OD to afford a 29 mM solution (3 : 1 v/v, respectively) and the reaction was monitored by ^1H NMR spectroscopy at room temperature (Fig. 1 and Fig. S1†). Model compound **1** was fully converted to products in 40 h, liberating $ArNH_2$ **2** in ∼61% yield and ArOH **3** in ∼72% yield. The release of $ArNH_2$ **2** and ArOH **3** follows first order kinetics with half-lives of $t_{1/2} = 4$ and 6 h, respectively. Release kinetics are roughly 2-fold faster compared to our previously studied 5-aryloxy-substituted 2-furylcarbinol derivative, which we attribute to increased electron density on the aryloxy group due to the methoxy substituent. Another set of peaks was observed in the ^1H NMR spectrum that corresponds to the formation of a minor product resulting from rebound of the liberated nucleophilic $ArNH_2$ **2** onto the quinone methide derived from the self-immolative linker (Fig. S2†). As expected,[26] the formation of this rebound product is concentration dependent and is not observed in reactions with a lower substrate concentration of 20 μM (Fig. S3†), on the same order of the mechanophore concentration in typical mechanochemical activation experiments (*vide infra*). Taking the amount of rebound product into account, the total yield of $ArNH_2$ **2** is ∼93% in the experiment described by Fig. 1, illustrating the efficiency with which fragmentation of the furfuryl carbamate occurs. The slightly lower yield of ArOH **3** compared to $ArNH_2$ **2** suggests that incomplete fragmentation or other side reactions occur in the second step involving the self-immolative linker. Nevertheless, the relatively high release yields of both cargo molecules and the similar release kinetics of $ArNH_2$ **2** and ArOH **3** highlight the potential of this platform for mechanically triggered dual payload release.

Encouraged by the reactivity of the small molecule model compound incorporating a self-immolative linker, we next set out to investigate mechanically triggered dual cargo release from a masked 2-furylcarbinol mechanophore incorporated into a polymer. Density functional calculations using the

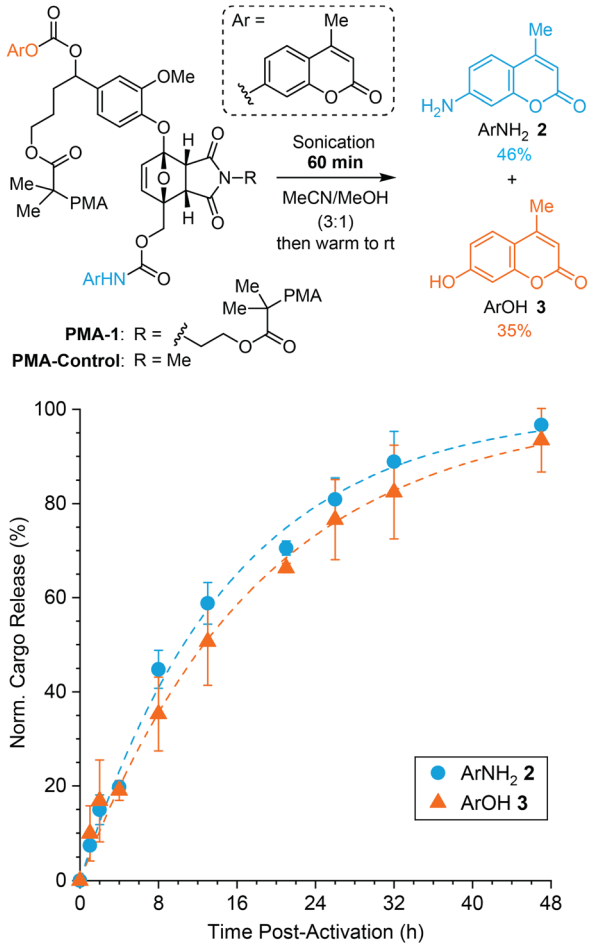

Fig. 2 Mechanically triggered release of $ArNH_2$ **2** and ArOH **3** upon ultrasound-induced mechanochemical activation of **PMA-1** (2 mg mL^{-1} in 3 : 1 MeCN/MeOH). Cargo release was measured at room temperature beginning immediately after sonication of **PMA-1** for 60 min as characterized by quantitative HPLC. The dashed lines are fits to simple first order kinetics. The initial value was subtracted from each measurement and the data were normalized to the plateau value of the fitted curve to highlight the relative release rates of each payload. Error bars represent standard deviation from three replicate experiments.

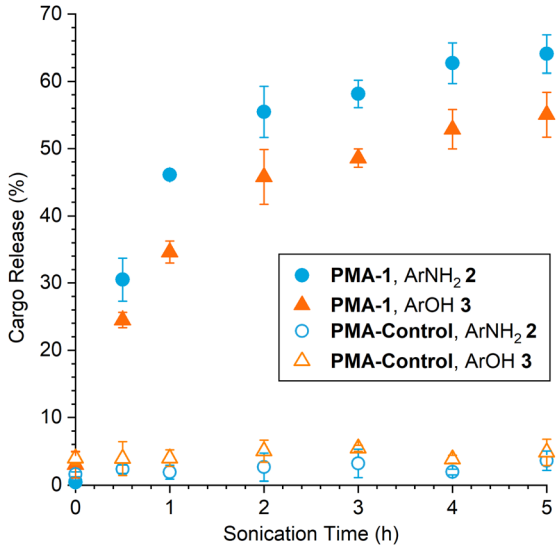

Fig. 3 Mechanically triggered release of $ArNH_2$ **2** and ArOH **3** from **PMA-1** and **PMA-Control** subjected to varying durations of sonication. Cargo release was quantified by HPLC after incubation at room temperature for 48 h following sonication. Error bars represent standard deviation from three replicate experiments.

constrained geometries simulate external force (CoGEF) technique[33,34] predict the desired formal retro-[4 + 2] cycloaddition reaction of the target furan–maleimide adduct upon mechanical extension leading to the formation of the intended 5-aryloxy-substituted 2-furylcarbinol derivative (Fig. S4†). Therefore, the synthesis commenced from compound **4**, which was prepared in three steps from vanillin in 50% overall yield (Scheme 2, see the ESI† for details). Next, deprotection and nucleophilic substitution with 5-bromofurfural afforded furaldehyde **5** in 74% yield over the two steps. Esterification of the primary alcohol proceeded *via* carbodiimide coupling with α-bromoisobutyric acid to produce **6** in 44% yield. Reduction of the aldehyde with sodium borohydride at −40 °C followed by a [4 + 2] cycloaddition reaction with a pre-functionalized maleimide dienophile at room temperature produced *endo*-Diels–Alder adduct **7** in 51% yield after isolation *via* silica gel chromatography. Finally, the two cargo molecules were installed in a two-step sequence, first by selective functionalization of the primary alcohol with a coumarin isocyanate followed by installation of the second cargo with a coumarin chloroformate to generate bis-initiator **8** in 48% yield, which was then employed in the controlled radical polymerization of methyl acrylate with Cu wire/Me_6TREN in DMSO[35] to afford **PMA-1** (M_n = 106 kDa; $Đ$ = 1.13) containing a chain-centered mechanophore. A similar synthetic procedure using *N*-methylmaleimide was used to prepare chain-end functional polymer **PMA-Control** (M_n = 98 kDa; $Đ$ = 1.15, see the ESI† for details). The electron rich aryloxy substituent imparts substantial thermal stability to Diels–Alder adduct **7**.[27] Heating a solution of **7** in toluene-d_8 at 70 °C for 5 and 24 h results in only ~5 and 25% retro-Diels–Alder reaction, respectively, while no retro-Diels–Alder reaction was observed at room temperature over several weeks (Fig. S5 and S6†).

The mechanochemical reactivity of the mechanophore in **PMA-1** was evaluated using pulsed ultrasonication (1 s on/1 s off, 12–13 °C, 20 kHz, 30% amplitude, 16.4 W cm^{-2}) and cargo release was characterized by high-performance liquid chromatography (HPLC). To compare the kinetics of payload release from **PMA-1** with that from isolated small molecule model compound **1**, a 2 mg mL^{-1} solution of **PMA-1** in 3 : 1 MeCN/MeOH was subjected to ultrasonication for 60 min (sonication "on" time), and then cargo release was quantified at regular time intervals from aliquots of the solution incubated at room temperature (Fig. 2). We note that fluorescence spectroscopy can also be used to selectively quantify the formation of $ArNH_2$ **2** (but not ArOH **3**), which provided similar results and additional confidence in the HPLC measurements (see the ESI† for additional details). The release of $ArNH_2$ **2** from the mechanically unmasked 2-furylcarbinol intermediate generated from **PMA-1** occurs with a half-life of $t_{1/2}$ = 11 h, which is slightly shorter

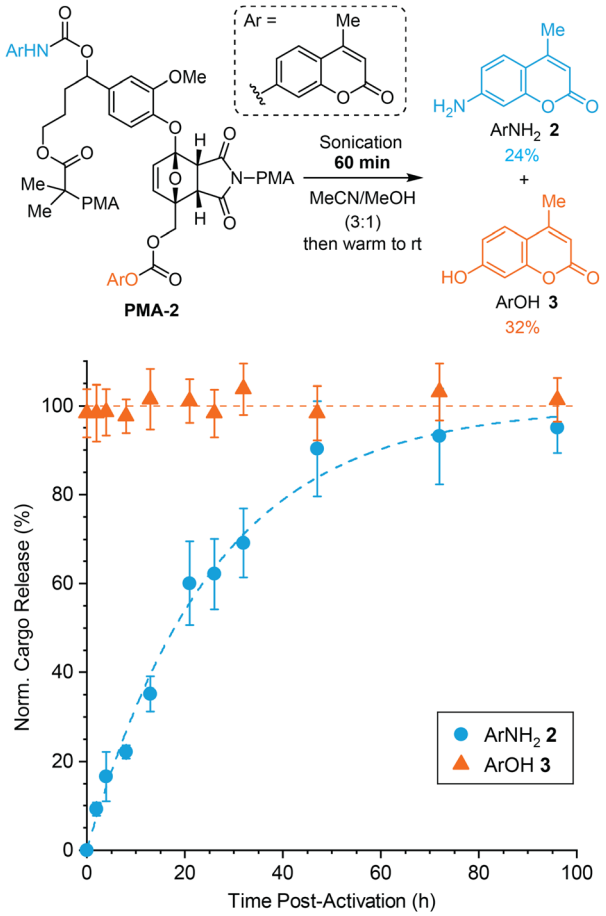

Fig. 4 Mechanically triggered release of $ArNH_2$ **2** and ArOH **3** upon ultrasound-induced mechanochemical activation of **PMA-2** (2 mg mL^{-1} in 3 : 1 MeCN/MeOH). Cargo release was measured at room temperature beginning immediately after sonication of **PMA-2** for 60 min and characterized by quantitative HPLC. The data for $ArNH_2$ **2** were normalized to the plateau value of the fit to simple first order kinetics (dashed blue line), while the data for ArOH **3** was normalized to the average percent release across all measurements. Error bars represent standard deviation from three replicate experiments.

than our previously reported substrate with a non-self-immolative tyrosol linker ($t_{1/2}$ = 15 h),[27] consistent with the more electron rich aryloxy group derived from vanillin. Notably, the release of the second payload, ArOH **3**, occurs with a similar half-life of $t_{1/2}$ = 13 h under these conditions. Normalized cargo release is plotted in Fig. 2 to highlight the relative release rates of each payload. These results are qualitatively consistent with the release kinetics measured for small molecule model compound **1** and demonstrate the rapid fragmentation–elimination–decarboxylation cascade of the self-immolative linker that follows initial furfuryl carbamate decomposition leading to the release of the first cargo, $ArNH_2$ **2** (see Fig. 1).

Increasing the duration of ultrasonication leads to a predictable increase in payload release from **PMA-1** with increasing mechanophore conversion, achieving average yields of 64% for $ArNH_2$ **2** and 55% for ArOH **3** after 5 h of sonication (Fig. 3). Aliquots were periodically removed from the sonicated solution of **PMA-1** over the course of the experiment and incubated at room temperature for 48 h to allow the complete fragmentation of the mechanically generated furan intermediate before quantifying cargo release by HPLC. Consistent with the experimental results for the decomposition of isolated small molecule **1**, the amount of released $ArNH_2$ **2** is higher than ArOH **3** at every point in the reaction, again suggesting that the second fragmentation process involving the self-immolative linker is slightly less efficient than initial fragmentation of the mechanically unmasked 2-furylcarbinol derivative. Gel permeation chromatography was also used to determine changes in molar mass resulting from polymer chain scission. Rather than the typical bimodal evolution of molar mass that is characteristic of mid-chain scission,[36] we observed a continuous shift in the average molar mass upon ultrasonication of **PMA-1** (Fig. S7†). This trend is similar to results with our original aryloxy-substituted masked 2-furylcarbinol mechanophore,[27] which we attribute to the relatively broad molar mass distribution (*i.e.*, $Đ$ > 1.1) that increases the competition between mechanophore activation and nonspecific chain scission and ultimately results in lower mechanophore activation efficiency.[37,38] Importantly, negligible cargo release was observed upon ultrasonication of **PMA-Control** that incorporates the cargo-loaded mechanophore at the polymer chain end, which is not subjected to mechanical force, confirming the mechanical origin of payload release from **PMA-1** (Fig. 3).

To further probe the dual release mechanism and also demonstrate the ability to systematically modulate the kinetics of payload release, we prepared polymer **PMA-2** (M_n = 120 kDa, $Đ$ = 1.35) incorporating a chain centered mechanophore in which the two cargo molecules, $ArNH_2$ **2** and ArOH **3**, are conjugated at opposite positions compared to **PMA-1** (Fig. 4). Based on the proposed fragmentation mechanism and the pronounced difference in reactivity between the furfuryl carbonate and furfuryl carbamate,[26,32] we would expect that the release of ArOH **3** will occur rapidly, with much slower release of the second payload, $ArNH_2$ **2**, conjugated to the self-immolative linker (Fig. S8†). A modified synthetic protocol compared to **PMA-1** was required due to challenges forming the carbonate selectively at the primary alcohol on Diels–Alder adduct **7**. Instead, $ArNH_2$ **2** was first installed *via* carbamate formation on the secondary alcohol of furfural derivative **6**, which was then carried through a similar synthesis as the one illustrated in Scheme 2 (see the ESI† for details). To evaluate the kinetics of cargo release from **PMA-2**, a 2 mg mL^{-1} polymer solution in 3 : 1 MeCN/MeOH was subjected to similar ultrasonication conditions as above for 60 min and cargo release was subsequently monitored at room temperature using HPLC (Fig. 4). Again, normalized cargo release is plotted in Fig. 4 to highlight the relative rates of release of each payload. The non-normalized data are provided in Fig. S9.† As anticipated, the release of ArOH **3** reached a maximum prior to the first measurement and remained essentially constant over time, indicating that furfuryl carbonate decomposition occurs essentially immediately following mechanical activation of the mechanophore.[27] In contrast, the release of the second cargo, $ArNH_2$ **2**, occurred with a significantly longer half-life of $t_{1/2}$ = 18 h. After 60 min of

sonication, $ArNH_2$ **2** was released in 24% yield and ArOH **3** was released in 32% yield. Here, the even higher dispersity of **PMA-2** compared to **PMA-1** likely contributes to the diminished cargo release yields after the same extent of sonication, resulting from lower mechanophore conversion under similar conditions. We speculate that the higher dispersity may reflect the closer proximity of the carbamate group to the benzylic stereocenter on the bis-initiator. Similar to the results above, the release of the first cargo molecule from the initially generated furfuryl carbonate is again slightly more efficient than the release of the second cargo conjugated to the self-immolative linker. Notably, however, the dramatic difference in cargo release kinetics observed for **PMA-2** compared to **PMA-1** highlights the ability to fine-tune the relative release profiles based on the identity of the cargo and the attachment position on the mechanophore scaffold. Moreover, these results provide additional support for the stepwise fragmentation mechanism, indicating that expulsion of the self-immolative aryloxy group occurs after initial decomposition of the mechanically generated 2-furylcarbinol derivative. Importantly, negligible cargo release was observed after incubating **PMA-2** in 3 : 1 MeCN/MeOH for 96 h at room temperature (Fig. S10†), fully consistent with control experiments demonstrating the stability of the primary carbonate under these conditions and supporting the mechanical origin of payload release.[27] The ability to precisely control the relative release profiles of two different drug molecules, for example, is a unique attribute afforded by this mechanophore design, making it potentially suitable for applications in schedule-dependent combination therapies with enhanced therapeutic efficacy.[39,40]

Conclusions

We have designed a novel mechanophore based on a masked 5-aryloxy-substituted 2-furylcarbinol derivative incorporating a self-immolative spacer facilitating the mechanically triggered release of two distinct molecular payloads. The mechanophore design leverages a unique fragmentation pathway involving the initial decomposition of a mechanochemically unveiled 2-furylcarbinol derivative to release the first payload followed by a second fragmentation process resulting in expulsion of the aryloxy substituent. Installation of a judiciously designed aryloxy spacer capable of self-immolation *via* a 1,6-elimination mechanism enables the release of a second payload molecule from a single mechanophore. Notably, we demonstrate that the relative release rates of the two cargo molecules are varied over a wide range based on both the reactivity of the payload/linker group and the position of conjugation to the mechanophore. By simply switching the attachment positions of two model payloads, mechanically triggered release occurs either concurrently or sequentially, resulting in remarkably different release profiles. The selectivity, modularity, and tunable release kinetics afforded by this mechanophore design provide a promising platform for a variety of potential applications including real-time monitoring of drug distribution, combination chemotherapy, and even dual catalysis.

Data availability

All data is available in the paper and/or ESI.†

Author contributions

Y.-L. T., T. Z., and M. J. R. designed the research. Y.-L. T. performed the experiments. Y.-L. T., T. Z., and M. J. R. analyzed the data. Y.-L. T. and M. J. R. wrote the manuscript. M. J. R. provided guidance during all stages of the project.

Conflicts of interest

There are no conflicts to declare.

Acknowledgements

Financial support from the Arnold and Mabel Beckman Foundation through a Beckman Young Investigator Award and the National Institute of General Medical Sciences of the National Institutes of Health (R35GM150988) is gratefully acknowledged. We thank the Center for Catalysis and Chemical Synthesis of the Beckman Institute at Caltech for access to equipment. Y.-L. T. gratefully acknowledges the J. Yang & Family Foundation for a first year fellowship at Caltech. M. J. R. gratefully acknowledges the Alfred P. Sloan Foundation for a Sloan Research Fellowship and the Camille and Henry Dreyfus Foundation for a Camille Dreyfus Teacher-Scholar Award.

References

1 R. Groote, R. T. M. Jakobs and R. P. Sijbesma, Mechanocatalysis: forcing latent catalysts into action, *Polym. Chem.*, 2013, **4**, 4846–4859.
2 M. A. Ghanem, A. Basu, R. Behrou, N. Boechler, A. J. Boydston, S. L. Craig, Y. Lin, B. E. Lynde, A. Nelson, H. Shen and D. W. Storti, The role of polymer mechanochemistry in responsive materials and additive manufacturing, *Nat. Rev. Mater.*, 2021, **6**, 84–98.
3 Y. Zhang, J. Yu, H. N. Bomba, Y. Zhu and Z. Gu, Mechanical Force-Triggered Drug Delivery, *Chem. Rev.*, 2016, **116**, 12536–12563.
4 M. M. Caruso, D. A. Davis, Q. Shen, S. A. Odom, N. R. Sottos, S. R. White and J. S. Moore, Mechanically-Induced Chemical Changes in Polymeric Materials, *Chem. Rev.*, 2009, **109**, 5755–5798.
5 M. K. Beyer and H. Clausen-Schaumann, Mechanochemistry: The Mechanical Activation of Covalent Bonds, *Chem. Rev.*, 2005, **105**, 2921–2948.
6 J. Li, C. Nagamani and J. S. Moore, Polymer Mechanochemistry: From Destructive to Productive, *Acc. Chem. Res.*, 2015, **48**, 2181–2190.
7 M. Stratigaki and R. Göstl, Methods for Exerting and Sensing Force in Polymer Materials Using Mechanophores, *ChemPlusChem*, 2020, **85**, 1095–1103.
8 Y. Yao, M. E. McFadden, S. M. Luo, R. W. Barber, E. Kang, A. Bar-Zion, C. A. B. Smith, Z. Jin, M. Legendre, B. Ling,

D. Malounda, A. Torres, T. Hamza, C. E. R. Edwards, M. G. Shapiro and M. J. Robb, Remote control of mechanochemical reactions under physiological conditions using biocompatible focused ultrasound, *Proc. Natl. Acad. Sci. U. S. A.*, 2023, **120**, e2309822120.

9 B. A. Versaw, T. Zeng, X. Hu and M. J. Robb, Harnessing the Power of Force: Development of Mechanophores for Molecular Release, *J. Am. Chem. Soc.*, 2021, **143**, 21461–21473.

10 C. E. Diesendruck, B. D. Steinberg, N. Sugai, M. N. Silberstein, N. R. Sottos, S. R. White, P. V. Braun and J. S. Moore, Proton-Coupled Mechanochemical Transduction: A Mechanogenerated Acid, *J. Am. Chem. Soc.*, 2012, **134**, 12446–12449.

11 Y. Lin, T. B. Kouznetsova and S. L. Craig, A Latent Mechanoacid for Time-Stamped Mechanochromism and Chemical Signaling in Polymeric Materials, *J. Am. Chem. Soc.*, 2020, **142**, 99–103.

12 M. B. Larsen and A. J. Boydston, "Flex-Activated" Mechanophores: Using Polymer Mechanochemistry To Direct Bond Bending Activation, *J. Am. Chem. Soc.*, 2013, **135**, 8189–8192.

13 H. Shen, M. B. Larsen, A. G. Roessler, P. M. Zimmerman and A. J. Boydston, Mechanochemical Release of N-Heterocyclic Carbenes from Flex-Activated Mechanophores, *Angew. Chem., Int. Ed.*, 2021, **60**, 13559–13563.

14 Y. Sun, W. J. Neary, Z. P. Burke, H. Qian, L. Zhu and J. S. Moore, Mechanically Triggered Carbon Monoxide Release with Turn-On Aggregation-Induced Emission, *J. Am. Chem. Soc.*, 2022, **144**, 1125–1129.

15 S. Nijem, Y. Song, R. Schwarz and C. E. Diesendruck, Flex-activated CO Mechanochemical Production for Mechanical Damage Detection, *Polym. Chem.*, 2022, **13**, 3986–3990.

16 M. Di Giannantonio, M. A. Ayer, E. Verde-Sesto, M. Lattuada, C. Weder and K. M. Fromm, Triggered Metal Ion Release and Oxidation: Ferrocene as a Mechanophore in Polymers, *Angew. Chem., Int. Ed.*, 2018, **57**, 11445–11450.

17 Y. Sha, Y. Zhang, E. Xu, Z. Wang, T. Zhu, S. L. Craig and C. Tang, Quantitative and Mechanistic Mechanochemistry in Ferrocene Dissociation, *ACS Macro Lett.*, 2018, 1174–1179.

18 Y. Zhang, Z. Wang, T. B. Kouznetsova, Y. Sha, E. Xu, L. Shannahan, M. Fermen-Coker, Y. Lin, C. Tang and S. L. Craig, Distal conformational locks on ferrocene mechanophores guide reaction pathways for increased mechanochemical reactivity, *Nat. Chem.*, 2021, **13**, 56–62.

19 Y. Lu, H. Sugita, K. Mikami, D. Aoki and H. Otsuka, Mechanochemical Reactions of Bis(9-methylphenyl-9-fluorenyl) Peroxides and Their Applications in Cross-Linked Polymers, *J. Am. Chem. Soc.*, 2021, **143**, 17744–17750.

20 F. Yang, T. Geng, H. Shen, Y. Kou, G. Xiao, B. Zou and Y. Chen, Mechanochemical Release of Fluorophores from a "Flex-activated" Mechanophore, *Angew. Chem., Int. Ed.*, 2023, e202308662.

21 S. Huo, P. Zhao, Z. Shi, M. Zou, X. Yang, E. Warszawik, M. Loznik, R. Göstl and A. Herrmann, Mechanochemical bond scission for the activation of drugs, *Nat. Chem.*, 2021, **13**, 131–139.

22 Z. Shi, Q. Song, R. Göstl and A. Herrmann, Mechanochemical activation of disulfide-based multifunctional polymers for theranostic drug release, *Chem. Sci.*, 2021, **12**, 1668–1674.

23 Q. Hu, W. Sun, C. Wang and Z. Gu, Recent advances of cocktail chemotherapy by combination drug delivery systems, *Adv. Drug Delivery Rev.*, 2016, **98**, 19–34.

24 Z. Shi, Q. Song, R. Göstl and A. Herrmann, The Mechanochemical Release of Naphthalimide Fluorophores from β-Carbonate and β-Carbamate Disulfide-Centered Polymers, *CCS Chem.*, 2021, **3**, 2333–2344.

25 X. Hu, T. Zeng, C. C. Husic and M. J. Robb, Mechanically Triggered Small Molecule Release from a Masked Furfuryl Carbonate, *J. Am. Chem. Soc.*, 2019, **141**, 15018–15023.

26 X. Hu, T. Zeng, C. C. Husic and M. J. Robb, Mechanically Triggered Release of Functionally Diverse Molecular Payloads from Masked 2-Furylcarbinol Derivatives, *ACS Cent. Sci.*, 2021, **7**, 1216–1224.

27 T. Zeng, X. Hu and M. J. Robb, 5-Aryloxy substitution enables efficient mechanically triggered release from a synthetically accessible masked 2-furylcarbinol mechanophore, *Chem. Commun.*, 2021, **57**, 11173–11176.

28 C. C. Husic, X. Hu and M. J. Robb, Incorporation of a Tethered Alcohol Enables Efficient Mechanically Triggered Release in Aprotic Environments, *ACS Macro Lett.*, 2022, **11**, 948–953.

29 M. Shamis, H. N. Lode and D. Shabat, Bioactivation of Self-Immolative Dendritic Prodrugs by Catalytic Antibody 38C2, *J. Am. Chem. Soc.*, 2004, **126**, 1726–1731.

30 K. Haba, M. Popkov, M. Shamis, R. A. Lerner, C. F. Barbas III and D. Shabat, Single-Triggered Trimeric Prodrugs, *Angew. Chem., Int. Ed.*, 2005, **44**, 716–720.

31 M. Staderini, A. Gambardella, A. Lilienkampf and M. Bradley, A Tetrazine-Labile Vinyl Ether Benzyloxycarbonyl Protecting Group (VeZ): An Orthogonal Tool for Solid-Phase Peptide Chemistry, *Org. Lett.*, 2018, **20**, 3170–3173.

32 A. Alouane, R. Labruère, T. Le Saux, F. Schmidt and L. Jullien, Self-Immolative Spacers: Kinetic Aspects, Structure–Property Relationships, and Applications, *Angew. Chem., Int. Ed.*, 2015, **54**, 7492–7509.

33 M. K. Beyer, The mechanical strength of a covalent bond calculated by density functional theory, *J. Chem. Phys.*, 2000, **112**, 7307–7312.

34 I. M. Klein, C. C. Husic, D. P. Kovács, N. J. Choquette and M. J. Robb, Validation of the CoGEF Method as a Predictive Tool for Polymer Mechanochemistry, *J. Am. Chem. Soc.*, 2020, **142**, 16364–16381.

35 N. H. Nguyen, B. M. Rosen, G. Lligadas and V. Percec, Surface-Dependent Kinetics of Cu(0)-Wire-Catalyzed Single-Electron Transfer Living Radical Polymerization of Methyl Acrylate in DMSO at 25 °C, *Macromolecules*, 2009, **42**, 2379–2386.

36 K. L. Berkowski, S. L. Potisek, C. R. Hickenboth and J. S. Moore, Ultrasound-Induced Site-Specific Cleavage of Azo-Functionalized Poly(ethylene glycol), *Macromolecules*, 2005, **38**, 8975–8978.

37 Z. S. Kean, G. R. Gossweiler, T. B. Kouznetsova, G. B. Hewage and S. L. Craig, A Coumarin Dimer Probe of Mechanochemical Scission Efficiency in the Sonochemical Activation of Chain-Centered Mechanophore Polymers, *Chem. Commun.*, 2015, **51**, 9157–9160.

38 A. C. Overholts and M. J. Robb, Examining the Impact of Relative Mechanophore Activity on the Selectivity of Ultrasound-Induced Mechanochemical Chain Scission, *ACS Macro Lett.*, 2022, 733–738.

39 B. J. M. Braakhuis, V. W. T. R. van Haperen, M. J. P. Welters and G. J. Peters, Schedule-dependent therapeutic efficacy of the combination of gemcitabine and cisplatin in head and neck cancer xenografts, *Eur. J. Cancer*, 1995, **31**, 2335–2340.

40 M. J. Lee, A. S. Ye, A. K. Gardino, A. M. Heijink, P. K. Sorger, G. MacBeath and M. B. Yaffe, Sequential Application of Anticancer Drugs Enhances Cell Death by Rewiring Apoptotic Signaling Networks, *Cell*, 2012, **149**, 780–794.